HHS Public Access

Author manuscript

BJU Int. Author manuscript; available in PMC 2018 January 01.

Published in final edited form as:

BJU Int. 2017 January ; 119(1): 177–184. doi:10.1111/bju.13555.

The Origins of Urinary Stone Disease: Upstream mineral formations initiate downstream Randall's plaque

Ryan S. Hsi,
Department of Urology, University of California San Francisco, Can Francisco, CA

Krishna Ramaswamy,
Department of Urology, University of California San Francisco, Can Francisco, CA; Department of Urology, Kaiser Permanente Medical Center, Oakland, CA

Sunita P. Ho*, and
Division of Biomaterials and Bioengineering, Department of Preventive and Restorative Dental Sciences, School of Dentistry, University of California San Francisco, San Francisco, CA

Marshall L. Stoller*
Department of Urology, University of California San Francisco, San Francisco, CA

Abstract

Objectives—To describe a new hypothesis for the initial events leading to urinary stones. A biomechanical perspective on Randall's plaque formation through form and function relationships is applied to functional units within the kidney we have termed the "medullo-papillary complex" – a dynamic relationship between intratubular and interstitial mineral aggregates.

Materials and Methods—A complete MEDLINE search was performed to examine the existing literature regarding the anatomical and physiological relationships in the renal medulla and papilla. Sectioned human renal medulla with papilla from radical nephrectomy specimens were imaged using a high resolution micro X-ray computed tomography. The location, distribution, and density of mineral aggregates within the medullo-papillary complex were identified.

Results—Mineral aggregates were observed proximally in all specimens within the outer medulla of medullary complex and were intratubular. Distal interstitial mineralization at the papillary tip corresponding to Randall's plaque was not observed until a threshold of proximal mineralization was observed. Mineral density measurements suggest varied chemical compositions between the proximal intratubular (330 mg/cc) and distal interstitial (270 mg/cc) deposits. A review of the literature revealed distinct anatomical compartments and gradients across

Corresponding Author: Sunita P. Ho, Ph.D., Division of Biomaterials and Bioengineering, Department of Preventive and Restorative Dental Sciences, School of Dentistry, HSW813 513, Parnassus Avenue, HSW8, University of California San Francisco, San Francisco, CA 94143, sunita.ho@ucsf.edu.

*Both authors contributed equally to this work as co-senior authors

Conflicts of Interest Statement

The authors of this manuscript certify that they have no affiliations with or involvement in any organization or entity with any financial interested in the subject matter or materials discussed in this manuscript.

the medullo-papillary complex that supports the empirical observations that mineralization proximally triggers distal Randall's plaque formation.

Conclusion—The initial stone event is initiated by intratubular mineralization of the renal medullary tissue leading to the interstitial mineralization that is observed as Randall's plaque. We base this novel hypothesis on a multiscale biomechanics perspective involving form and function relationships, and empirical observations. Additional studies are needed to validate this hypothesis.

Keywords

kidney; urolithiasis; calcification; physiologic; urinary tract physiology

Introduction

Whale and dolphin kidneys are shaped in the likeness of a lung consisting of many smaller kidney bean-shaped alveoli-like renal units that resemble a small human kidney.(1) Desert rats compared to their counterparts that live in damp environments have nearly half as many nephrons and reduced filtration surface area for water economy, yet the overall shape and compartments of the kidney remain preserved.(2) The shape and size of the kidney among species varies depending on the overall size of the animal and its functional needs, yet the archetype of the renal functional unit is conserved. These and other form-function relationships provide insight into the mechanisms of physiologic and pathologic states within organ systems such as the kidney.

At the smallest scale, the functional unit of the kidney is considered to be the nephron. However for urologists, the functional units most clinically relevant are the 8–12 paraboloid structures within a kidney visualized during endoscopy consisting of the renal papilla and medulla, which we term the "medullo-papillary complex". This structure is observed in the majority of mammalian renal systems, with some kidneys being uni-papillary systems while others contain multiple papillae.

Regardless of the number of papilla, the paraboloid shape guides the various lengths of the tubules along its axis that are responsible for adjusting the final urinary filtrate. We propose that this shape is a critical element and is predisposed to form biominerals. While the absolute number and density of tubules is uncertain, these functional units can be impaired due to changes in environmental stimuli. The shifts in stimuli can in turn cause functional impairment and favor stone formation while maintaining adequate urinary excretion. It is this process that we would like to apply to the kidney: environmental stimuli help define form, and that form guides function. (3, 4)

Current thought holds that the Randall's plaque serves as a nidus on which stones form for idiopathic calcium oxalate stone formers.(5) However, the formation of Randall's plaques, and subsequent renal stones, is not well understood. We propose that Randall's plaque formation at the tip of the medullo-papillary complex is not the headwaters but a downstream event. We hypothesize that mineral formation begins within the tubules in the proximal renal medulla and prompts a cascade of events that culminate to the distally

observed interstitial mineralization leading to Randall's plaque formation in the papilla. We will demonstrate this by coupling the unique form of the human renal medullo-papillary complex to its function and providing evidence from high-resolution X-ray microscopy.

Historical and current perspectives on kidney stone formation: Homage to Randall's Theory

Randall originally proposed that calcium deposition at the tips of renal papillae was the precursor to renal stones and described the characteristic "plaque" as calcium phosphate, not within the tubular lumen, but "invading and replacing interstitial tissue".(6, 7) He also observed that Randall plaques increase with age. He theorized that upon these plaques, calcium phosphate and calcium oxalate stones grow and eventually break off and subsequently become urinary tract stones that often are symptomatic. This implies that the Randall's plaque is at the intersection between papillary mineralization and urinary tract stone *in vivo.*

Developments in endoscopic technology have demonstrated Randall's plaque in a majority of calcium stone formers.(8) The fractional plaque coverage in idiopathic calcium oxalate stone formers is higher than that in non-stone formers,(9) and the percentage of plaque coverage correlates with the number of stones formed.(10) Furthermore, endoscopically observed stones are often attached to renal papilla at sites of plaque.(11)

Advanced imaging modalities have been used to characterize the origins of Randall's plaque from biopsy specimens from the papillary tip.(12) The identified mineral deposits are located within the interstitium of the renal papillary tip and often are thought to originate from the basement membrane of the thin loops of Henle. Plaques are thought to originate as spherical deposits of apatite as small as 50 nm in the interstitial matrix and are proposed as the beginnings of later plaque development that Randall had observed.(13) However, because these observations have been obtained from papillary biopsies, the upstream events that lead to Randall's plaque formations have not been examined and are not understood.

Medullo-papillary Complex Form and Function

The medullo-papillary complex is shaped like a paraboloid (a parabola rotated about its long axis) extending into the minor calyx of the collecting system (Figure 1). Each of the 8–12 medullo-papillary complexes within the kidney is comprised of three anatomically distinct medullary zones based on the segments of the nephron: Zone 1 consists of the outer stripe of the outer medulla, Zone 2 the inner stripe of the outer medulla, and Zone 3 the inner medulla (Figure 1A).(2, 14)

Longitudinally, nephrons can be divided into two major populations of long and short nephrons based on the length of the loops of Henle (Figure 2).(2, 15) Compared to long loop nephrons, short loops are limited to Zones 1 and 2 and have no thin ascending limb segments. The long loop nephrons form 180-degree bends predominantly in Zones 2 and 3 as they travel deeper towards the tip of papilla and become fewer in number, which affects urine concentrating ability.(16) The paraboloid shape mandates that there are short

peripherally located nephrons and long centrally located nephrons in the medullo-papillary complex.

Blood vessels lie in close proximity to these loops to facilitate countercurrent exchange of ions and water in the transverse direction.(17) As the descending vasa rectae enter Zone 1 at various levels, they dive longitudinally with little or no transverse branching towards the tip of the papilla, where they each make a 180-degree U-bend and split into 2–3 ascending vasa rectae. From the base to the tip of the medullo-papillary complex, both the lumen diameter and the pressure within the vasa rectae decrease as they approach the tip of the papilla.(18) Surrounding the descending vasa rectae are 1–3 layers of smooth muscle cells in Zone 2, which disappear as they approach the tip of the papilla where pericytes replace them.(17–19) Pericytes are known to have mesenchymal stem-cell like properties including osteogenic phenotype.(20) Within Zone 3, the smooth muscle cells disappear, suggesting that deeper blood flow is not regulated by contractile mechanisms.(21) Non-fenestrated endothelium of the descending vasa rectae becomes fenestrated after the U-bend to become the ascending vasa rectae, affecting water and small solute reabsorption along the length of the medullo-papillary complex.(17)

Transversely, the medullo-papillary complex is divided into anatomically specific functional compartments that generate concentration gradients (Figure 2).(14) Zone 2 is divided into *vascular bundles* and *interbundle* regions.(17, 22) The vascular bundles contain the descending vasa rectae and ascending vasa rectae that travel exclusively together with no branching.(22) The longest descending vasa rectae emerge at the tip of the papilla into Zone 3 where there is higher interstitial osmolarity, and are located more centrally within these vascular bundles.(23) Within the interbundle regions are the thin limbs and collecting ducts. The vascular bundles and interbundle regions have minimal communication because the descending thin limbs and collecting ducts are located within the center of the interbundle region, and the water-impermeable thick ascending limbs lie at the margin of the vascular bundles.(22)

In contrast, Zone 3 is divided into *collecting duct clusters* with large diameters and *vascular bundles* of narrow diameters (Figure 2).(21) The collecting duct clusters predominately contain the collecting ducts, ascending thin limbs, and possibly water-impermeable descending thin limbs. The vascular clusters are dominated by ascending and descending vasa rectae, and contain water-permeable descending thin limbs. Whereas the descending thin limbs associate closely with the collecting ducts in Zone 2, they anatomically transition to lie distant from collecting ducts in Zone 3. The physical separation of these anatomically-specific compartments in addition to their individual structural variations, contribute to regions with specific concentration gradients that occur not only along the length of the tubules, but also in the transverse direction.(24, 25)

Pressure gradients exist along the medullo-papillary complex (Figure 3).(19) Longitudinally, pressure within Zone 1 is higher than in Zone 3 and drives perfusion and tubular flow. Among the descending vasa rectae, the larger diameter vessels are located within the centers of vascular bundles and travel towards the tip of the renal papilla.(19) From proximal to distal, the long looped nephrons associated with the descending vasa rectae centrally have

higher pressure gradients than the short looped nephrons located peripherally in the medullo-papillary complex.

Chemical gradients within the medullo-papillary complex facilitate the formation of concentrated and dilute urine (Figure 3). The medullary osmotic gradient is generated by active NaCl reabsorption from the thick ascending limb in Zones 1 and 2, maintained by the descending thin limb (water permeable but low permeability to Na and urea) and ascending thin limb (high Na permeability, low urea permeability, and impermeable to water) segments in Zone 3, and augmented by passive urea and water reabsorption in the collecting ducts.(19, 26) Adding to the complexity of these gradients are the spatial relationships of the tubules and vessels within the compartments, generating local concentration gradients.(17, 21) Finally, tissue oxygen gradients present within the medullo-papillary complex create areas of relative hypoxemia in the thick ascending limbs and medullary collecting ducts due to the relatively high metabolic demands of the channels in these zones.(23, 27, 28)

Proposed Mechanism of Biomineralization from Proximal to Distal in the Medullo-papillary Complex

The rate of flow within the medullo-papillary complex can be described by Poiseuille's equation, where the flow rate is directly proportional to the pressure gradient along the tube, fourth power of the radius, and is inversely proportional to the fluid viscosity and tubule length. The fluid velocity near the wall is minimal compared to the centerline velocity due to the resistance of flow from the tubular wall.(29)

These fundamental principles can be applied at two levels: 1) at the level of the medullo-papillary complex, and 2) at the level of the tubules within the complex. Taken together, pressure gradients within the peripherally oriented, shorter tubules within the paraboloid complex are lower than the centrally located tubules (Figure 4). Given, the lower pressure gradients along with lower velocities at the tubular walls, over a lifespan, particulates can accumulate along the walls of these shorter tubules in Zones 1 and 2, akin to a stream where the floating leaves accumulate at the edges of the bank of a stream. As these shorter, peripheral tubules become progressively obstructed, there is a decrease in the functional volume of the overall complex. In other words, the functional "volume" of tubules is reduced once the peripheral tubules are devoid of flow. As such, more flow is diverted centrally, which changes the internal pressure and subsequently the "stiffness" of the medullo-papillary complex specifically at the interface where the shorter tubules end and the longer tubules continue to traverse into Zone 3. At this interface between Zones 2 and 3 could be a mechanoresponsive switch that is turned "on" due to a shift in form (as the functional radius decreases to the fourth power, the pressure within the medullo-papillary complex increases significantly), and fluid is shunted to the centrally located tubules.

Once this mechanoresponsive switch is turned on, a cascade of biological events is triggered distally. The centrally located smaller diameter yet pressurized vasa rectae and loops of Henle develop a differential in the hoop or circumferential strain at the interface between Zones 2 and 3 and plausibly could leak into Zone 3. At this interface, we hypothesize that integrins facilitate transfer of change in stiffness of the extracellular matrix to intracellular

compartments, and that this differential in hoop strain could predominantly impact pericytes located near the tip of the medullo-papillary complex. Pericytes are known to have progenitor-like phenotype and can differentiate into an osteoblastic lineage making the environment conducive to sequester inorganic ions – the early stages of cell-based biomineralization.(20) It is through this postulate that we explain the formation of the apatite substrate: the Randall's plaque. A second proposed mechanism involves elevated hydrostatic pressure in the vasa rectae driving solutes into the interstitium through the fenestrated endothelium, which overwhelms resorption capability of the tubular cells in Zone 3, leading to accumulation of interstitial biominerals.

Evidence for Mineralization in the Medullo-papillary Complex: Materials and Methods

In an IRB-approved study, radical nephrectomy specimens for renal tumor (n=12) were sectioned to isolate the medullo-papillary complex in grossly normal appearing kidney tissue, sufficiently far away from the malignancy in question. No kidneys with urothelial tumors were examined. All subjects had no prior history of stone disease. Specimens placed in a centrifuge tube in 50% ethanol and were mounted inside a calibrated microcomputed tomography unit (MicroXCT-200, Carl Zeiss X-ray Microscopy, Pleasanton, CA). Specimens were imaged at 4X magnification, 40kV, 8W, 5s exposure time, pixel size 5.01μm, and with 2000 image projections. Reconstructed tomograms (using XMReconstructor software) were processed to determine mineral densities in milligrams per cubic centimeter and were related to surrounding tubular structures.

Results

In all specimens, micro-CT demonstrated streaks and aggregates of mineralized regions in Zones 1 and 2 within the medullo-papillary complex that correspond to more peripherally located tubules (Figure 5A). Mineralization was predominately intratubular in location. Only the specimens with greater volume of proximal, intratubular mineralization were observed to have distal interstitial mineralization near the papilla (Figure 5B, 5C).

This suggests that proximal mineralization could precede distal mineralization. In other words, interstitial deposits were observed in association with the central nephrons in the inner medulla at the papillary tip, and never in isolation without the more proximal peripheral intratubular mineralization. Furthermore, mean mineral densities of the proximal mineralization were higher (330 mg/cc) than that of the distal papillary region (270mg/cc). The volume fraction of mineralization was distinct proximally compared to distally (0.2% vs 4.5%). These two mineralization processes occur not only in separate locations, but their mineral densities and plausibly their chemical compositions could differ. It is with this preliminary evidence that we postulate the pathophysiological cascade with the earliest mineralization being proximal and distant from the traditional Randal plaque.

Discussion

All filters over time become less efficient with the accumulation of minerals. The kidney is a biofilter undergoing constant reclamation of solutes and excretion of waste over a multi-decade period. Here, we identify evidence that mineralization within the medullo-papillary complex occurs in the absence of overt stone disease, and that greater amounts of proximal intratubular mineralization is accompanied with greater amounts of distal interstitial mineralization. Though visualization of Randall's plaque is a first sign of urinary stone disease endoscopically, the mineralization process within the medullo-papillary complex is already well advanced when these plaques are appreciated. For the first-time calcium stone former, the expression of stone disease may represent the accumulation of lifestyle choices over prior decades. In a way, it is too late. Stones represent the end-product of a long cascade of events.

However, an appreciation that the etiology of Randall's plaque is initiated more proximally within the medullo-papillary complex may focus the development of therapeutics that would help modulate or slow the mineralization process. For instance, based on Poiseuille's equation, viscosity of the tubular or blood flow might be modulated to allow improved flow and decelerate the process of mineral deposition. It also has been observed that not all who have Randall's plaques form kidney stones, as 19% of the normal population have grossly visible plaque,(6, 7) which is higher than reported kidney stone prevalence.(30) Forming kidney stones may therefore require a "two-hit" process, with Randall's plaque as a predisposed insult.

Additional studies are needed to confirm these observations, but challenges remain. Age-related processes over the long-term are difficult to study. A suitable animal model to study renal mineralization is yet to be identified, as there is no established animal model of Randall's plaque formation, and most animal models have uni-papillary systems as opposed to the multi-papillary system found in humans. Despite these challenges, recent advances in micro- and nano-resolution imaging techniques and modeling microfluidics may provide more insights into the biomineralization process than originally appreciated.

Conclusion

Biomechanical approaches to renal physiology and pathophysiology can add insight to the current paradigm on the initiation of nephrolithiasis. The urinary tract was designed to transport fluids, not solids. We now realize that once a calculus becomes dislodged from the papilla, it is too late. This detached, free-floating stone now has the threat of growth, obstruction, and causing symptoms to its host. While mechanisms within the urinary milieu such as nucleation and supersaturation contribute to stone maturation within the collecting system, it is the pathologic changes that occur at the tissue level within the parenchyma that may be fundamentally more important.

Acknowledgments

This research was supported by contracts NIH NIDDK – 1P20DK100863 (MLS); NIH NIDCR - R01DE022032 (SPH); NIH/NCRR S10RR026645, (SPH).

References

1. Abdelbaki YZ, Henk WG, Haldiman JT, Albert TF, Henry RW, Duffield DW. Macroanatomy of the renicule of the bowhead whale (Balaena mysticetus). Anat Rec. 1984; 208(4):481–90. [PubMed: 6731857]
2. Bankir L, de Rouffignac C. Urinary concentrating ability: insights from comparative anatomy. Am J Physiol. 1985; 249(6 Pt 2):R643–66. [PubMed: 3934988]
3. Bradley SE. Jean Redman Oliver: in context. Kidney international. 1974; 5(2):77–95. [PubMed: 4592671]
4. Bradley SE, Laragh JH, Wheeler HO, Macdowell M, Oliver J. Correlation of Structure and Function in the Handling of Glucose by the Nephrons of the Canine Kidney. J Clin Invest. 1961; 40(7):1113–31. [PubMed: 16695865]
5. Matlaga BR, Coe FL, Evan AP, Lingeman JE. The role of Randall's plaques in the pathogenesis of calcium stones. The Journal of urology. 2007; 177(1):31–8. [PubMed: 17161996]
6. Randall A. Papillary pathology as a precursor of primary renal calculus. The Journal of urology. 1940; 44:580.
7. Randall A. The Origin and Growth of Renal Calculi. Ann Surg. 1937; 105(6):1009–27. [PubMed: 17856988]
8. Low RK, Stoller ML. Endoscopic mapping of renal papillae for Randall's plaques in patients with urinary stone disease. The Journal of urology. 1997; 158(6):2062–4. [PubMed: 9366312]
9. Kuo RL, Lingeman JE, Evan AP, et al. Urine calcium and volume predict coverage of renal papilla by Randall's plaque. Kidney international. 2003; 64(6):2150–4. [PubMed: 14633137]
10. Kim SC, Coe FL, Tinmouth WW, et al. Stone formation is proportional to papillary surface coverage by Randall's plaque. The Journal of urology. 2005; 173(1):117–9. discussion 9. [PubMed: 15592050]
11. Matlaga BR, Williams JC Jr, Kim SC, et al. Endoscopic evidence of calculus attachment to Randall's plaque. The Journal of urology. 2006; 175(5):1720–4. discussion 4. [PubMed: 16600740]
12. Kuo RL, Lingeman JE, Evan AP, et al. Endoscopic renal papillary biopsies: a tissue retrieval technique for histological studies in patients with nephrolithiasis. The Journal of urology. 2003; 170(6 Pt 1):2186–9. [PubMed: 14634375]
13. Evan AP, Lingeman JE, Coe FL, et al. Randall's plaque of patients with nephrolithiasis begins in basement membranes of thin loops of Henle. J Clin Invest. 2003; 111(5):607–16. [PubMed: 12618515]
14. Lemley KV, Kriz W. Cycles and separations: the histotopography of the urinary concentrating process. Kidney international. 1987; 31(2):538–48. [PubMed: 3550222]
15. Kriz W. Structural organization of the renal medulla: comparative and functional aspects. Am J Physiol. 1981; 241(1):R3–16. [PubMed: 7018270]
16. Layton HE. Distribution of Henle's loops may enhance urine concentrating capability. Biophys J. 1986; 49(5):1033–40. [PubMed: 3708088]
17. Pallone TL, Turner MR, Edwards A, Jamison RL. Countercurrent exchange in the renal medulla. Am J Physiol Regul Integr Comp Physiol. 2003; 284(5):R1153–75. [PubMed: 12676741]
18. Evans RG, Eppel GA, Anderson WP, Denton KM. Mechanisms underlying the differential control of blood flow in the renal medulla and cortex. J Hypertens. 2004; 22(8):1439–51. [PubMed: 15257161]
19. Pallone, TL.; Cao, C. Renal Cortical and Medullary Microcirculations. In: Alpern, Robert J.; Hebert, Steven C.; Moe, Orson W., editors. Seldin and Giebisch's The Kidney. 5. Academic Press; 2013. p. 803-857.Print. 2013
20. Collett GD, Canfield AE. Angiogenesis and pericytes in the initiation of ectopic calcification. Circ Res. 2005; 96(9):930–8. [PubMed: 15890980]
21. Wei G, Rosen S, Dantzler WH, Pannabecker TL. Architecture of the human renal inner medulla and functional implications. Am J Physiol Renal Physiol. 2015; 309(7):F627–37. [PubMed: 26290371]

22. Ren H, Gu L, Andreasen A, et al. Spatial organization of the vascular bundle and the interbundle region: three-dimensional reconstruction at the inner stripe of the outer medulla in the mouse kidney. Am J Physiol Renal Physiol. 2014; 306(3):F321–6. [PubMed: 24305474]
23. Pannabecker TL, Layton AT. Targeted delivery of solutes and oxygen in the renal medulla: role of microvessel architecture. Am J Physiol Renal Physiol. 2014; 307(6):F649–55. [PubMed: 25056344]
24. Pannabecker TL, Dantzler WH. Three-dimensional lateral and vertical relationships of inner medullary loops of Henle and collecting ducts. Am J Physiol Renal Physiol. 2004; 287(4):F767–74. [PubMed: 15187004]
25. Pannabecker TL, Dantzler WH. Three-dimensional architecture of inner medullary vasa recta. Am J Physiol Renal Physiol. 2006; 290(6):F1355–66. [PubMed: 16380456]
26. Pannabecker TL. Comparative physiology and architecture associated with the mammalian urine concentrating mechanism: role of inner medullary water and urea transport pathways in the rodent medulla. Am J Physiol Regul Integr Comp Physiol. 2013; 304(7):R488–503. [PubMed: 23364530]
27. Fry BC, Edwards A, Sgouralis I, Layton AT. Impact of renal medullary three-dimensional architecture on oxygen transport. Am J Physiol Renal Physiol. 2014; 307(3):F263–72. [PubMed: 24899054]
28. Brezis M, Rosen S, Silva P, Epstein FH. Selective vulnerability of the medullary thick ascending limb to anoxia in the isolated perfused rat kidney. J Clin Invest. 1984; 73(1):182–90. [PubMed: 6690477]
29. Fung, YC. Biomechanics Circulation. 2. Springer Science; 1997. Physical Principles of Circulation; p. 1-22.
30. Scales CD Jr, Smith AC, Hanley JM, Saigal CS. Urologic Diseases in America P. Prevalence of kidney stones in the United States. Eur Urol. 2012; 62(1):160–5. [PubMed: 22498635]

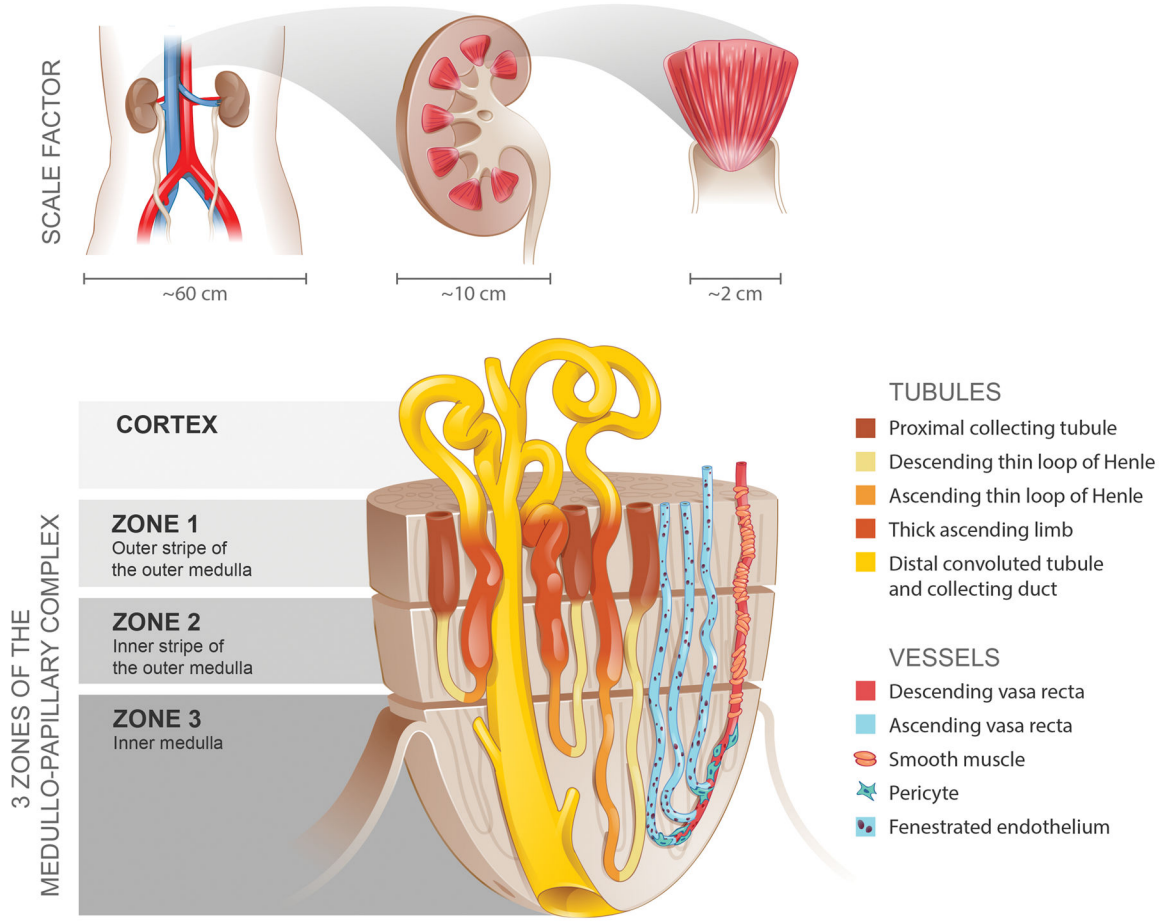

Figure 1.

The medullo-papillary complex. A total of 8–12 paraboloid complexes are contained within each human kidney. Each complex can be separated into three zones distinguished by distinct segments of the loop of Henle. There are short and long looped nephrons and vessels. Owing to the paraboloid geometry of the medullo-papillary complex, shorter looped nephrons and vessels are contained in the periphery, and the longest looped nephrons and vessels are located centrally. Non-fenestrated descending vasa rectae are surrounded by layers of smooth muscle, in contrast to the ascending vasa rectae comprised of fenestrated endothelium. Within Zone 3, a transition occurs where pericytes replace smooth muscle.

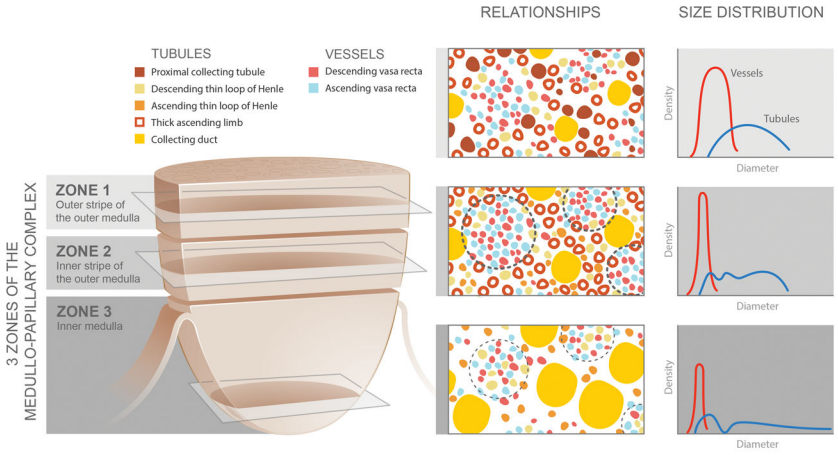

Figure 2.

Spatial relationships and size distributions of the tubules and vessels within the medullo-papillary complex. From Zone 1 to Zone 2, the ascending and descending vasa recta become organized into vascular bundles (dotted line) and interbundle regions. In Zone 3, the descending thin limbs join the vascular bundles (light dotted line), and these are separate from collecting duct clusters. Collecting ducts grow larger in diameter towards zone 3 and coalesce to form the 6–12 ducts of Bellini. These anatomically specific compartments contribute to radial and axial concentration gradients along the course of the complex.

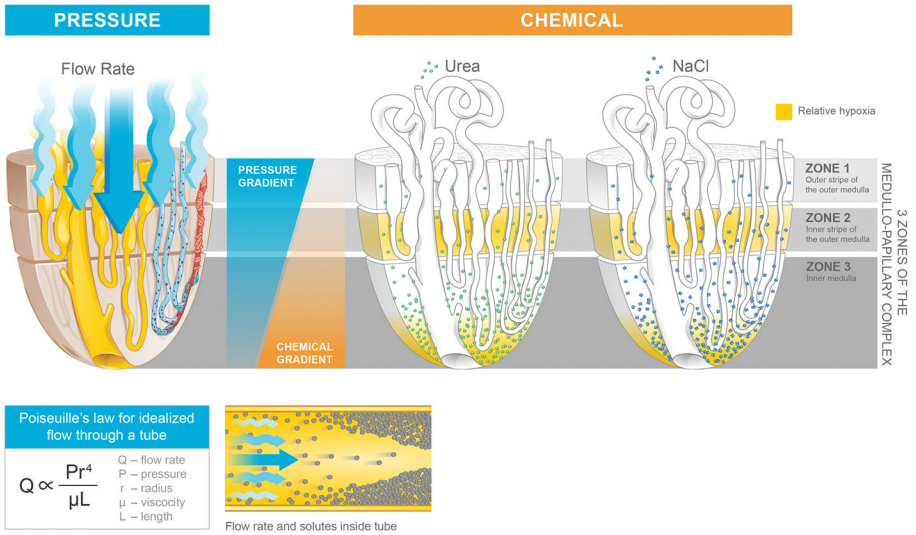

Figure 3.

Medullo-papillary function is characterized by pressure and chemical gradients. Pressure gradients are present from Zone 1 to Zone 3. Due to the paraboloid form of the complex, larger diameter vasa recta are located centrally within the vascular bundles and have greater pressure gradients and flow rates than in the peripherally located vasa recta. Poiseuille's law relates flow rate as proportional to pressure and radius to the fourth power, and inversely proportional to fluid viscosity and tube length. Within each tube, velocity of fluid is highest at the centerline, but decreases near the wall due to resistance. Over time, within a concentrated fluid, solutes are expected to accumulate along the walls. From Zone 1 to Zone 3, an increasing osmolarity gradient, contributed by primarily sodium salts and urea, generates the urine concentrating ability through the countercurrent exchange. Areas vulnerable to hypoxic injury include the tip of the Zone 3, and Zone 2 because of the metabolically active thick ascending limbs and their relative physical separation from the descending vasa recta.

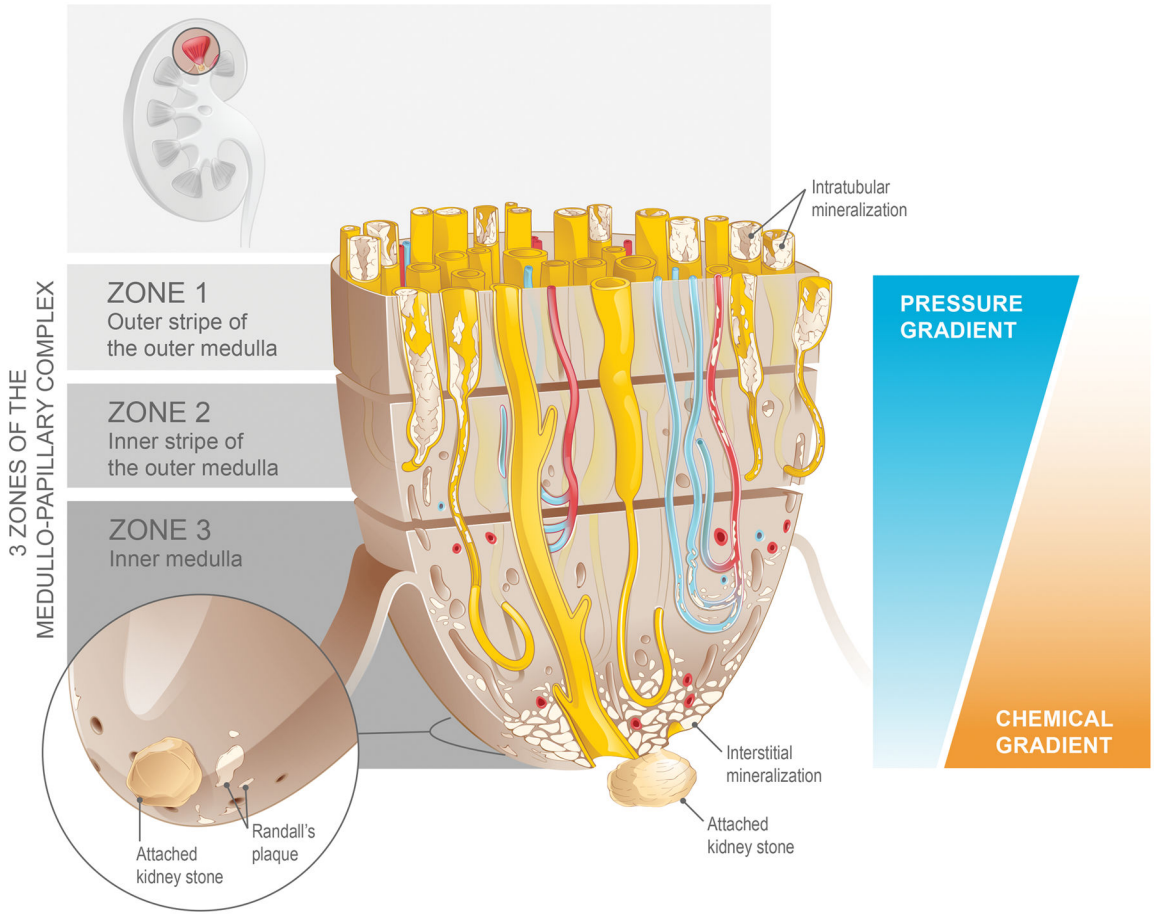

Figure 4.

Biomineralization of the medullo-papillary complex leading to Randall's plaque. Over time, lower pressure gradients in the peripheral tubules relative to the centrally located tubules lead to intratubular mineralization within Zones 1 and 2. The functional volume of the complex gradually decreases, and at a certain threshold, the change in pressure gradient drives a mechanoresponsive switch that leads to interstitial mineralization in Zone 3. The accumulation of biominerals in the interstitial space eventually becomes endoscopically visible as Randall's plaque, the foundation for a future urinary tract stone.

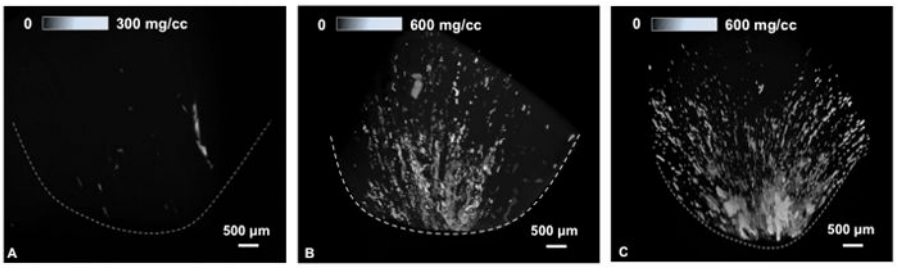

Figure 5.

Micro-computed tomography of human medullo-papillary complex. From left to right, a comparison of increasing mineralization is detectable in 3 subjects. Streaks and aggregates of mineralized regions in Zones 1 and 2 are predominantly intratubular in location. With greater proximal mineralization, distal interstitial mineralization becomes apparent. Upper scale bars represent gradients in mineral densities within the medullo-papillary complex.